Vol. 13(18), pp. 250-256, 30 November, 2018
DOI: 10.5897/IJPS2018.4741
Article Number: 38E860459528
ISSN: 1992-1950

http://www.academicjournals.org/IJPS

ACADEMIC JOURNALS
expand your knowledge

International Journal of Physical Sciences

Full Length Research Paper

Mathematical modeling and numerical simulation for the formation process of nanofilms

M. M. Aish

Department of Physics, Faculty of Science, Menoufia University, Menoufia, Egypt.

Received 28 May, 2018; Accepted 27 November, 2018

This study applied a generalized model to describe and optimize the formation process of nanofilms from their polymeric solutions. Through this model, one can optimize the concentration of the solvent in the polymeric solution, the appropriate geometric dimensions as well as the nanofilm formation speed. A comparison of this model with experimental data has revealed some similarities and differences in the solidification and evaporation processes of the solvent. The yield strength and plasticity were deeply studied using numerical simulation for polypolymer nanofilms when subjected to a tensile deformation along the <001> direction.

Key words: Polypolymer, linear polymers, rheological equation of state, tensile deformation, polymer nanofilm.

INTRODUCTION

The yield strength and plasticity were deeply studied using numerical simulation for poly-polymer nanofilms when subjected to a tensile deformation. The use of mathematical modeling in the design and manufacture of products made of polymer materials has several advantages, which include quality management capabilities of polymer products and solutions of optimization of production tasks. Its basis is a mathematical model, which should be simple and at the same time reflect all the features of the process under investigation. One common treatment processes in production of polymeric materials is a polymeric nanofilm. In the industry, plastic nanofilm used is primarily done through polymer melt extrusion method (Silagy et al., 1998; Seay and Baird, 2009). This method is suitable for molding polymeric materials that do not melt when exposed to thermal degradation. The polymer melt is extruded through an extruder, after the release of that nanofilm in radiation falls on the cooling drum. As a result, the film movement from the extruder comes to cooling of the drum, the change of width and thickness when this film is unevenly stretched leads to “neck effect”. Since these processes occur simultaneously, with their mathematical modeling there must be a joint decision of equations for velocity, pressure and heat transfer (Kajiwara et al., 2003). For polymers whose melting point is higher than the temperature of their thermal decomposition, to obtain the so-called nanofilms polymer solution irrigation method should be applied (Ito et al., 2003). This method consists of three main stages: preparation of molding a specific concentration of the polymer solution through a spinneret, watering it on a polished surface (endless belt or drum), solvent removal (evaporation or by using the spin bath). It is used for

E-mail: mohamedeash2@yahoo.com.

stress relief, as well as improving physical and mechanical characteristics of the nanofilms produced in the molding process used heat treatment, binary or biaxial orientation.

In particular, not depending on the method for producing a solid liquid transition leads to uneven nanofilm structure change of geometric dimensions of the sample, which ultimately leads to the appearance of "neck effect". In both cases, the molding process is accompanied by relaxation and phase transition; when a film melt by solidification of the liquid film structure due to heat transfer processes, and by the solution - mass transfer. The process of obtaining a film of the polymer solution is inherently more complex because of a two-component system. In the molding conditions is an increase in polymer concentration, which leads to a sharp increase in the viscosity of the polymer system. Thus, when designing mathematical models polymeric nanofilm forming processes should be considered, particularly inherent features in each preparation process.

Polymer nanofilms are of great technological interest. They have potential applications in photoelectrical and photovoltaics (Akhgari et al., 2006; Gang et al., 2006; Wang et al., 2001; Starostenkov and Aish, 2014). They have been successfully synthesized, using various methods including electrochemistry, solution chemical reactions, and self-catalysis thermal evaporation (Akhgari et al., 2006).

Feng et al. (2006) have studied the mechanical properties of nanowires using nano indentation. On the other hand, Wang et al., (2001), using transmission electron microscopy, have studied the mechanical properties of silicon carbide-silica biaxial nanowires, and their structural transformation between a biaxial and coaxial configuration. The origin of such remarkable properties of some nanostructures is still unclear. Aish et al. (Starostenkov and Aish, 2013; Aish and Starostenkov, 2015; Aish and Starostenkov, 2013; Mohammed and Mikhail, 2016) have showed that the mechanical properties of Ni nanowires are highly dependent on the size, shape as well as the atomic vacancies in the nanowire and nanofilms.

Polypolemer nanofilms are of great technological interest. They have potential applications in photoelectrical and photovoltaics (Xu et al., 2000; Tans et al., 1997; Woo et al., 2002). They have been successfully synthesized using various methods including electrochemistry, solution chemical reactions, and self-catalysis thermal evaporation (Michalet et al., 2005).

Mechanical characterization of Polypolemer nanofilms is quite essential for deep understanding of their functionality as well as for the possibility of modeling and engineering new useful materials based on them.

Aiming at understanding the mechanical properties of Polypolemer nanofilms, molecular dynamics simulation was applied to characterize structural transformations that took place in the nanofilms when subjected to uniaxial stress.

Figure 1 shows a schematic representation of the nanofilm deformation process when subjected to a uniaxial tension. It is evident that the deformation process starts with the appearance of atomic domains, where the atoms in each domain displace collectively towards some preferred directions.

Mechanical characterization of polymer nanofilms is quite essential for deep understanding of their functionality as well as for the possibility of modeling and engineering new useful materials based on them.

Mathematical model

The work to find steady tensile stresses during use generalized rheology model in (20), the parameters of which are known concentration of functions.

$$\sigma_{ik} = -p\delta_{ik} + 3\frac{\eta_0}{\tau_0}a_{ik}; \qquad (1)$$

$$\frac{d}{dt}a_{ik} - \nu_{ij}a_{jk} - \nu_{kj}a_{ji} + \frac{1+(\kappa-\beta)I}{\tau_0}a_{ik} = \frac{2}{3}\gamma_{ik} - 3\frac{\beta}{\tau_0}a_{ij}a_{jk},$$

Where, σ_{ik} is the stress tensor; p is the hydrostatic pressure; η_0 and τ_0 is the initial values of the shear viscosity and relaxation time; ν_{ik} is the tensor of velocity gradients; a_{ik} is the symmetric tensor of the second anisotropy rank; I is the first invariant tensor anisotropy; $\gamma_{ik} = \frac{1}{2}(\nu_{ik} + \nu_{ki})$ – summarized tensor of velocity gradients; κ, β is the phenomenological parameters of the model, taking into account the equations of the dynamics of macromolecules change in size and shape of the molecular coil. Quantities η_0 and τ_0 depends on the polymer concentration in the system, which means that these values are changed upon solvent evaporation and must be set depending on the experiment. Values κ, β can be assumed apparently as constant.

In addition, rheological model was tested for adequacy by calculating the overlap of small oscillating fluctuations in a simple shear flow in parallel and orthogonal to the direction of shear (Giannikopoulos, 1998). In carrying out the numerical experiment obtained, it was dependent on the stress tensor of velocity gradients and from time to time, which allowed calculations of the components of the complex shear modulus, dynamic viscosity and the angle of the dynamic loss; depending on the frequency of the driving oscillations of shear rate and the number of Deborah (D_e). The dependences obtained are compared with experimental data taken from literature that showed qualitative agreement between theory and experiment. These results allow discussion on the adequacy of the rheological model (1), which allows its use in the

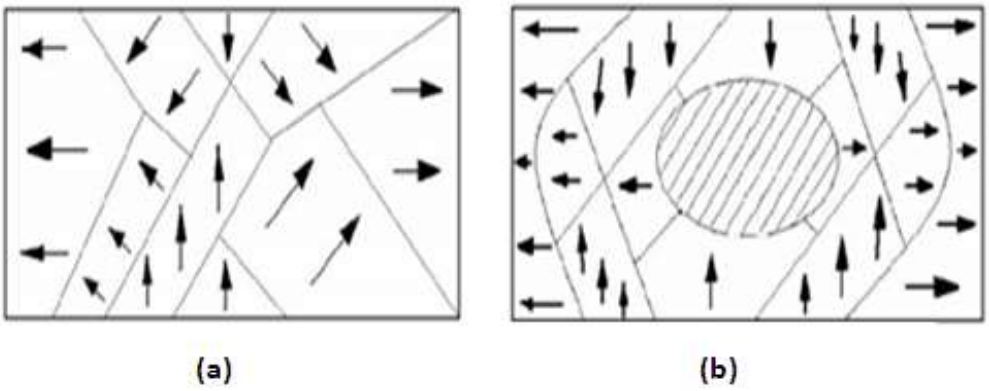

Figure 1. The appearance of structural domains where the atoms in each domain move collectively towards preferred directions (a) on the surface of the nanofilm and (b) at the core.

calculation of more complex movements than the realizable viscometers. For example, in (Sills et al., 2004; Overney, 1996; Overney, 1997), it was considered as a steady flow between parallel planes under a constant pressure drop. It is shown that the model 1 predicts a non-parabolic profile velocity and having a non-zero differential pressure in cross flow direction.

A model (1) was applied to describe the process of nanofilm forming polymer solution. Since in this case the velocity gradients are not known, then for the system of equations we add the equation of conservation of mass and momentum, which in Cartesian coordinates are of the form 24:

$$\frac{\partial v_x}{\partial x}+\frac{\partial v_y}{\partial y}+\frac{\partial v_z}{\partial z}=0,$$

$$\rho\left(\frac{\partial v_x}{\partial t}+v_x\frac{\partial v_x}{\partial x}+v_y\frac{\partial v_x}{\partial y}+v_z\frac{\partial v_x}{\partial z}\right)=\frac{\partial \sigma_{11}}{\partial x}+\frac{\partial \sigma_{12}}{\partial y}+\frac{\partial \sigma_{13}}{\partial z}$$

$$\rho\left(\frac{\partial v_y}{\partial t}+v_x\frac{\partial v_y}{\partial x}+v_y\frac{\partial v_y}{\partial y}+v_z\frac{\partial v_y}{\partial z}\right)=\frac{\partial \sigma_{21}}{\partial x}+\frac{\partial \sigma_{22}}{\partial y}+\frac{\partial \sigma_{23}}{\partial z}$$

$$\rho\left(\frac{\partial v_z}{\partial t}+v_x\frac{\partial v_z}{\partial x}+v_y\frac{\partial v_z}{\partial y}+v_z\frac{\partial v_z}{\partial z}\right)=\frac{\partial \sigma_{31}}{\partial x}+\frac{\partial \sigma_{32}}{\partial y}+\frac{\partial \sigma_{33}}{\partial z} \quad (2)$$

Where, v_x, v_y, v_z – velocities in x, y and z axis respectively; ρ – density. In case of registration of the evaporation, system (1, 2) must be supplemented by the transport equation for concentration:

$$\rho\left(\frac{\partial c}{\partial t}+v_x\frac{\partial c}{\partial x}+v_y\frac{\partial c}{\partial y}+v_z\frac{\partial c}{\partial z}\right)=\frac{\partial}{\partial x}\left(\lambda\frac{\partial c}{\partial x}\right)+\frac{\partial}{\partial y}\left(\lambda\frac{\partial c}{\partial y}\right)+\frac{\partial}{\partial z}\left(\lambda\frac{\partial c}{\partial z}\right) \quad (3)$$

Where c is the concentration of the solvent, λ - the diffusion coefficient.

Next, the problem of stationary when in the fixed coordinate system have time-dependent quantities was considered. In this case, it was noted that the nanofilm thickness can be quite small and the concentration of the nanofilm thickness was considered constant. The origin is put in the middle of the outlet of the spinneret, x-axis along the direction of motion of the nanofilm and look for depending only on the variable solution of 1 to 3.

$$v_x=u(x);\qquad c=c(x). \quad (4)$$

The kinematics process can be described in terms of the uniaxial stress, as in (Tsui and Pharr, 1999). In the case of steady flow, stretching the continuity equation becomes:

$$\rho\left(\frac{\partial V_x}{\partial x}+2\frac{\partial V_y}{\partial y}\right)+V_x\frac{\partial \rho}{\partial x}=0,$$

From which the one-dimensional approach was obtained:

$$\frac{\partial V_y}{\partial y}=-\frac{1}{2}\left(\frac{du}{dx}+\frac{ud\rho}{\rho dx}\right).\quad \text{And}\ \frac{d\rho}{dx}=(\rho_2-\rho_1)\frac{dc}{dx}$$

Where, ρ_1 - the density of the polymer, ρ_2 – solvent density, $\rho=(1-c)\rho_1+c\rho_2$-the average density. Then the system of equations (1-4) takes the form:

$$\rho u\frac{du}{dx}=3\frac{d}{dx}\left(\frac{\eta_0}{\tau_0}(a_{11}-a_{22})\right)$$

$$u\frac{da_{11}}{dx}-2\frac{du}{dx}a_{11}+\frac{1+(\kappa-\beta)(a_{11}+2a_{22})}{\tau_0}a_{11}=\frac{2du}{3dx}-3\beta a_{11}^2$$

$$\rho u\frac{dc}{dx}=\lambda\frac{d^2c}{dx^2}-\frac{\mu}{h}(c-c_0) \tag{5}$$

$$u\frac{da_{22}}{dx}+\left(\frac{du}{dx}+\frac{u(\rho_2-\rho_1)dc}{\rho dx}\right)a_{22}+\frac{1+(\kappa-\beta)(a_{11}+2a_{22})}{\tau_0}a_{22}=-\frac{1}{3}\left(\frac{du}{dx}+\frac{u(\rho_2-\rho_1)dc}{\rho dx}\right)-3\beta a_{22}^2$$

Where, C_0– Maximum solvent concentration in the environmental medium, μ– the diffusion coefficient of exchange with the environmental medium, h=S/P – The ratio of the cross-sectional area and the nanofilm to sectional perimeter ($h=\frac{ab}{2a+2b}=\frac{b}{2}$, thin films a≥b).

The last term in the equation for concentration allows for the evaporation of the solvent through the surface of the nanofilm. Typically, solvent density is close to the density of the polymer, and therefore this difference, apparently, does not significantly have effect. In this case, the system of Equations 5 can be written as:

$$\rho u\frac{du}{dx}=3\frac{d}{dx}\left(\frac{\eta_0}{\tau_0}(a_{11}-a_{22})\right)$$

$$u\frac{da_{11}}{dx}-2\frac{du}{dx}a_{11}+\frac{1+(\kappa-\beta)(a_{11}+2a_{22})}{\tau_0}a_{11}=\frac{2du}{3dx}-3\beta a_{11}^2$$

$$u\frac{da_{22}}{dx}-\frac{du}{dx}a_{22}+\frac{1+(\kappa-\beta)(a_{11}+2a_{22})}{\tau_0}a_{22}=-\frac{1}{3}\frac{du}{dx}-3\beta a_{22}^2$$

$$\rho u\frac{dc}{dx}=\lambda\frac{d^2c}{dx^2}-\frac{\mu}{h}(c-c_0) \tag{6}$$

The system of Equations 5 is a set of four ordinary differential equations, of the first order and the second order forms. Therefore, it should be complemented by five boundary conditions. Four of them can be put simply, when v_x these conditions are: $v_x(0)=v_0$; $v_x(l)=kv_0$, where k – Film stretch factor.

The concentration of the boundary conditions can be supplied as follows: $c(0)=c_1$; $c'(l)=0$. Where c_1 – the concentration of the polymer solution. The second condition is that the concentration of the polymer on the tape (cylinder) takes a steady-state value.

Additional conditions for the stress can be obtained by calculating the polymer fluid in the volume of spinneret, which is a complex task. To evaluate the Stress a_{22} and a_{33} with reference to the work of Xu et al. (2000), were obtained by the formula for the calculation of the plane-parallel flow under a constant differential pressure:

$$\overline{A}=\frac{\tau_0}{\eta_0}\frac{\partial p}{\partial x}$$

$$a_{yy}=-\frac{\beta}{12}\overline{A}^2(h-2y)^2;u(y)=\frac{\overline{A}}{2\tau_0}y(h-y) \tag{7}$$

These expressions lead to the average values for stress and speed:

$$\overline{a}_{yy}=\frac{1}{R}\int_0^h a_{yy}(y)dy=-\frac{\beta}{36}\overline{A}^2h^2;$$

$$\overline{u}=\frac{1}{R}\int_0^h u(y)dy=-\frac{\overline{A}h^2}{12} \tag{8}$$

In addition, there is $\overline{a}_{yy}=-\frac{4\beta}{h^2}\tau_0^2\overline{u}^2$

In case of a_{22}, h – film width that is sufficiently large, and therefore in a boundary condition take $a_{22}(0)=0$. The opposite situation is observed for a_{33}, where h – is the nanofilm thickness. If these expressions are use, $a_{33}\to-\infty$ will be obtained. Those obtained up to first explain this contradiction order in Tans et al. (1997), the expression for the velocity and pressure by K and β, and these expressions are not just for large pressure gradients. In Overney et al. (1997), the limit value was found for $a_{yy}=-5/17$, which should be taken as a boundary condition for $a_{33}(0)=-5/17$. Thus, any of these conditions can be taken as missing fifth conditions.

When you perform calculations on a model 6 is necessary to obtain an expression for the width of the nanofilm due to the rate of its formation. In case of the melt flow simulation, when the volume does not change, this is simply the Expression 4:

$$a(x) = a(0)\sqrt{\frac{u(0)}{u(x)}} \quad (9)$$

Solutions must take into account correction associated with solvent evaporation. Let $c_1 = c(0)$ – the solvent concentration at the outlet of spinneret $c_2 = c(x)$ – the solvent concentration at a point x.

Then $\frac{1-c_1}{1-c_2}\rho(0) = \frac{1-c_1}{1-c_2}\left((1-c_1)\rho_1 + c_1\rho_2\right)$ – the mass of the solution at the point x, and the relative change in volume due to the evaporation of the solvent would be:

$$\frac{V(x)}{V(0)} = \frac{1-c_1}{1-c_2}\frac{\left((1-c_1)\rho_1 + c_1\rho_2\right)}{\left((1-c_2)\rho_1 + c_2\rho_2\right)} \quad (10)$$

Where, $\rho_1 = \rho_2$ this expression can be written as: $\frac{V(x)}{V(0)} = \frac{1-c_1}{1-c_2}$

This expression leads the following relation between the width of the film, its speed and obtaining the concentration of the polymer system:

$\frac{a^2(x)u(x)}{a^2(0)u(0)} = \frac{1-c_1}{1-c_2}$ Or,

$$a(x) = a(0)\sqrt{\frac{1-c(0)}{1-c(x)}\cdot\frac{u(0)}{u(x)}} \quad . \quad (11)$$

Similarly, the dependence of the nanofilm thickness of its speed forming was found, changing the solvent concentration in the polymer system.

To perform calculations on the system of Equations 6 must be installed depending on the model parameters η_0 and τ_0 concentration. Such dependence can be found when processing the experimental data, and quite often, they are of the nature of power (Overney, 1997). Thus, solving one of the numerical methods for the system of Equations 6, taking into account (11), can be found not only a change in the geometric dimensions (width, thickness) forms a nanofilm; but also depending on the stress tensor, components are responsible for a number of consumer properties of the resulting nanofilm samples. It should also be investigated experimentally determined influence of rheological parameters on the character of the theoretical curves. In the absence of modulus-matching, shear stresses will concentrate at the interface (Tans et al., 1997), and potentially compromise film stability.

Yield strength of the nanofilm

To calculate the dynamics of the atomic structure was used molecular dynamics method using Morse pair potentials (Aish and Starostenkov, 2013):

$$\varphi_{KL}(r) = D_{KL}\beta_{KL}e^{-\alpha_{KL}r}\left[\beta_{KL}e^{-\alpha_{KL}r} - 2\right] \quad (12)$$

Where, α_{KL}, β_{KL}, D_{KL} – parameters defining the interaction between a pair of atoms, K and L; r – the distance between the atoms. The interaction between atoms limited to three first coordination spheres. The initial velocities of the atoms according to the Maxwell distribution set the temperature of the experiment. To keep T constant, thermostat Berendsen was applied with a frequency correction rate once 10^{-13} s (Berendsen et al., 1984).

The dimensions of the Polypolemer nanofilms used in the following simulations are set to be Lz =5 and Lx=Ly, changes from 5 to 90.

Figure 2 shows the yield stress– cross-section relations obtained from the simulations at room temperature. As can be seen, the figure was divided into three regions, 1st region at small cross-section the simulated stress decreased with increasing cross-section; 2nd region at intermediate cross-section the simulated stress constant with increasing cross-section; and 3rd region at high cross-section the simulated stress increases with increasing cross-section. Figure 3 shows a dramatical change in strength with increasing nanofilm cross-sectional area at the strain rate of $2\times10^7 s^{-1}$. This is a "smaller is softer" effect. The effect of "smaller is softer" occurs for the nanofilms with smaller cross-sectional area and the self-similar hardening effect occurs for those nanofilms with high cross-sectional area.

Slipping parts in nanofilms tacking place, formed substructural blocks at the boundaries between the blocks packing defects formed. Atoms on the boundaries between substructural units had HCP topology as nearest neighbors. During the plastic deformation sequentially shift occurs several near parallel {111} planes, which led to the appearance of the side faces of the band, consisting of parallel lines slip with angle 35-45° to the axis of tension (Figure 3).

The formation of shear bands indicates the formation of twins because of structural-energy transformations in the process of high-speed deformation, as shown in Figure 4a and b. At the end of plastic deformation, there has been an increase in the number of twins and their gradual destruction (Figure 4a). The number of atoms in the HCP topology nearest neighbors located in parallel planes (Figure b) was increased.

The current investigation shows the heterogeneity of plastic deformation of Polypolemer nanofilms. It is evident

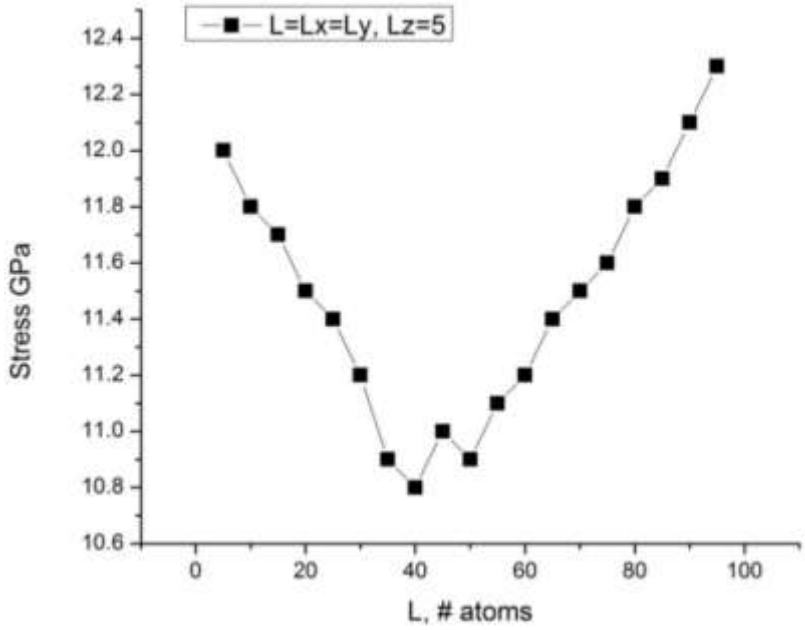

Figure 2. The simulated Yield strength of Polypolymer nanofilms as a function of nanofilm cross-sectional area at 300K.

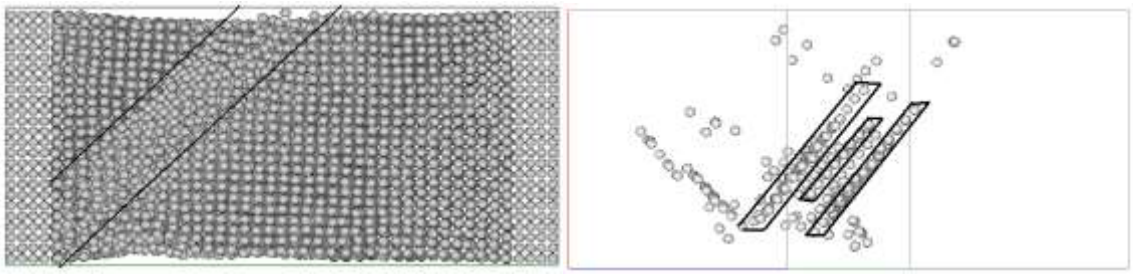

Figure 3. The strip of sliding parallel lines (a) and atoms with HCP topology of atoms as nearest neighbors in parallel planes, (b) at 58 ps at 300 K**.**

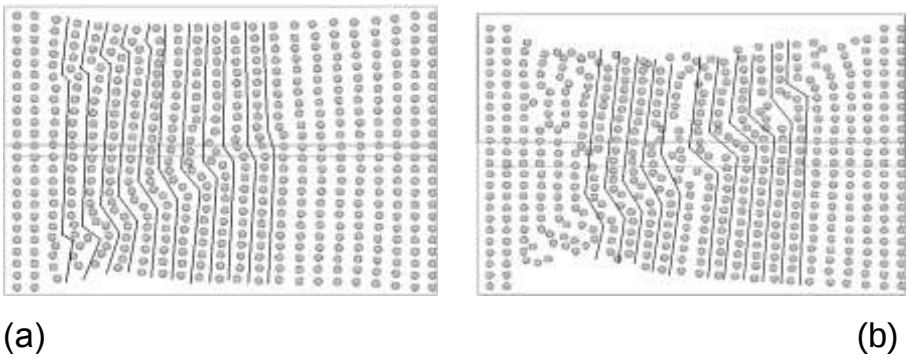

Figure 4. Atoms originally located in (110) plane of Polypolemer nanofilms in the direction of <001> at 58 ps (a) and 67 ps (b) at a temperature of 300 K.

that this deformation starts to occur at the central area of the film. It is found that structural elements in each domain depend on the orientation of the axis of compression. Moreover, the anisotropy of structural changes taking place in Polypolemer nanofilms does depend on its orientation. In particular, the development of plastic deformation stages in the direction <001> produces the formation of anti-phase boundaries and C-domains. C-domains form the plastic deformation.

Conclusion

This model has studied the isometric flows of real polymer liquids in the case of shear strain and uniaxial tension. In particular, it is shown that the state equation describes such effects observed in practice; how the viscosity of an anomaly, the first and second normal stress difference, viscosity increase the yield stress and tensile strain at its steady-state value. A good agreement was found between the theoretical and experimental curves in a wide range of deformation rates.

CONFLICT OF INTERESTS

The authors have not declared any conflict of interests.

REFERENCES

Aish MM, Starostenkov MM (2015). Modeling and simulation of ni nanofilm using morse pair potential Materials Physics and Mechanics 24:139-144.

Aish MM, Shatnawi MT, Starostenkov MD (2015). Characterization of strain-induced structural transformations in CdSe nanowires using molecular dynamics simulation. Materials Physics and Mechanics 24(4):403-409.

Aish MM, Starostenkov MM (2013). "Characterization of strain-induced structural transformations in CdSe nanowires using molecular dynamics simulation" Materials Physics and Mechanics 18(1):53-62.

Aish MM, Starostenkov MM (2016). AIP Conf. Proc. 1698, 040006 http://dx.doi.org/10.1063/1.4937842

Akhgari A, Faranmand F, Afrasiabi H, Sadeghi F, Vandamme T (2006). Permeability and swelling studies on free films containing inulin in combination with different polymethacrylates aimed for colonic drug delivery.European Journal of Pharmaceutical Sciences 28(4):307-314 Berendsen HJ, Postma JV, van Gunsteren WF, DiNola ARHJ, Haak JR (1984). Molecular dynamics with coupling to an external bath. The Journal of chemical physics 81(8):3684-3690.

Feng G, Nix WD, Yoon Y, Lee CJ (2006). A Study of the Mechanical Properties of Nanowires Using Nanoindentation. Journal of Applied Physics 99:074304.

Gang Feng, William D, Nix, Youngki Yoon, Cheol Jin Lee // J. Appl. Phys. 99, (2006) 074304.

Giannikopoulos AE Li, X, Bhushan B (1998). Measurement of fracture toughness of ultra-thin amorphous carbon films. Thin Solid Films, 315(1-2):214-221.

Ito H, Doi M, Isaki T, Takeo M, Yagi K (2003). 2D flow analysis of film casting process. Nihon Reoroji Gakkaishi 31(3):149-155.

Kajiwara T, Yamamura M, Asahina T (2003). Nihon Reoroji Gakkaishi Journal of Social Rheology 31:149-157.

Klein DL, Roth R, Lim AK, Alivisatos AP, McEuen PL (1997). A single-electron transistor made from a cadmium selenide nanocrystal. Nature 389(6652):699.

Michalet X, Pinaud FF, Bentolila LA, Tsay JM, S. J. J. L. DooseSJJJL, Li JJ, Sundaresan G Wu AM, Gambhir SS, Weiss S (2005). "Quantum dots for live cells, in vivo imaging, and diagnostics." science 307, no. 5709:538-544.

Overney RM, Leta DP, Fetters LJ; Liu Y, Rafailovich MH, Sokolov JJ (1996). vacuum. Science. Technology B14, 1276-1279.

Overney RM, Guo L, Totsuka H, Rafailovich M, Sokolov J, Schwarz SA (1996). Interfacially confined polymeric systems studied by atomic force microscopy. MRS Online Proceedings Library Archive 464.

Seay CW, Baird DG (2009). Sparse Long-chain Branching's Effect on the Film-casting Behavior of PE. International Polymer Processing, 24(1):41-49.

Silagy D, Demay Y, Agassant JF (1998) Axisymmetric entry flow of semi-dilute xanthan gum solutions: prediction and experiment. Journal of Non-Newtonian Fluid Mechanics 79:563-583.

Sills S, Overney RM, Chau W, Lee VY, Miller RD, Frommer J. Interfacial glass transition profiles in ultrathin, spin cast polymer films. The Journal of chemical physics. 2004 Mar 15; 120(11):5334-5338.

Starostenkov MD, Aish MM, Sitnikov AA, Kotrechko SA (2013). Deformation of different nickel nanowires at 300 K. Letters on Materials 3:180-183.

Starostenkov MD, Aish MM (2014). Effect of Length and Cross-Sectional Area on Ni3Fe Alloy Plasticity, Advanced Materials Research 1013:242-248.

Tans SJ, Devoret MH, Dai H, Thess A, Smalley RE, Geerligs LJ, Dekker C (1997). Individual single-wall carbon nanotubes as quantum wires. Nature 386(6624):474.

Tsui TY, Pharr GM (1999). Substrate effects on nanoindentation mechanical property measurement of soft films on hard substrates Journal of Material Resaerch Volume 14(1):292-301. https://doi.org/10.1557/JMR.1999.0042

Wang C, Shim M, Guyot-Sionnest P (2001). Electrochromic nanocrystal quantum dots. Science 291(5512):2390-2392.

Woo WK, Shimizu KT, Jarosz MV, Neuhauser RG, Leatherdale CA, Rubner MA, Bawendi MG (2002). Reversible Charging of CdSe Nanocrystals in a Simple Solid-State Device. Advanced Materials 14(15):1068-1071.

Xu D, Shi X, Gao G, Gui L, Tang Y (2000). Electrochemical Preparation of CdSe Nanowire Arrays, Journal of Physical Chemistry B 104, 5061 (2000).https://doi.org/10.1021/jp9930402